Journal of Materials Chemistry C

Accepted Manuscript

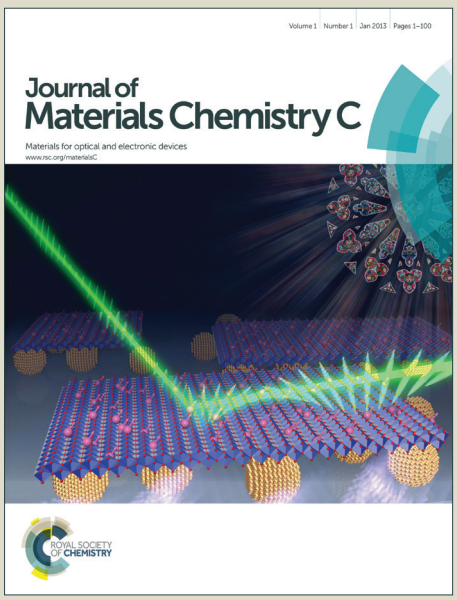

ROYAL SOCIETY OF CHEMISTRY

www.rsc.org/materialsC

Morphology inducing selective plasma etching for AlN nanocone arrays: Tip-size dependent photoluminescence and enhanced field emission properties

Weijie Sun, Yunlong Li, Yang Yang, Yunming Li, Changzhi Gu*, Junjie Li*

Beijing National Laboratory for Condensed Matter Physics, Institute of Physics.

Chinese Academy of Science, Beijing 100080, China

Abstract:

Bottom-up growth method has been a main way to form various AlN nanostructures but still existing many problems in uncontrollability and nonuniformity. Here we adopt firstly top-down plasma etching method to fabricate easily a large-area AlN nanocone arrays on magnetron sputtered (002) AlN films, and unique pebble-like array morphologies of AlN films surface induce greatly the whole selective plasma etching process without any masked process. The as-formed AlN nanocones have not only kept the crystalline oriented (002) and microstructure of original AlN film, but also had a good uniformity and controllability in height and density as well as tip-size. These AlN nancone arrays exhibited an intense broad ultraviolet emission centered at 3.26 eV and excellent field emission properties, and especially showing a tip-size dependent photoluminescence and field mission properties that were remarkably enhanced with decreasing the nanocone tip-size. Our results provide a promising route for controllable fabrication of AlN nanostructure and practical application of AlN-based various nanodevices in optoelectronics and vacuum-nanoelectronics.

Corresponding author. Tel.:+86-10-82649097; fax: +86-10-82648198.

E-mail address: jjli@aphy.iphy.ac.cn (J.J. Li) and czgu@iphy.ac.cn (C.Z.Gu)

1. Introduction

The III-nitride compounds have stimulated explosive research interest due to their unique properties and significant applications, such as optoelectronic devices in the visible and ultraviolet region [1]. Among these compounds, Aluminum nitride (AlN) exhibits high thermal conductivity, good electrical resistance, low dielectric loss, excellent mechanical strength and chemical stability [2, 3]. It is also known that AlN has a small electron affinity value ranging from negative to 0.6 eV, which means that electrons can be easily extracted from the surface to vacuum when an electric field is applied, thereby giving rise to a large field emission current density that is very attractive for field emission applications [4]. In addition, AlN exhibits the largest direct band gap of about ~6.2 eV among the hexagonal group III nitrides and it is thus crucial to produce solid-state light emitting devices [5]. In particular, AlN nanostructures have shown more novel physical and chemical properties than bulk AlN materials, such as small electron affinity, strong piezoelectricity, high surface acoustic wave (SAW) velocity and a tunable band gap, which are essential for applications in field emitters, flexible pulse-wave sensors and ultraviolet nanolasers.

Recently, various AlN nanostructures such as nanobelts[5], nanotubes[6], nanocones [7,8] and hierarchical comb-like structures [9], have been synthesized by different methods. Among these nanostructures, AlN nanocones have emerged as a new kind of one-dimensional nanostructures that is superior to other nanostructures in some aspects. For instance, it is found that the nanocones are more potential candidates for scanning probe and field emitters due to their radial rigidity, which eliminated poor signals and noise caused by mechanical or thermal vibration [10,11]. Up until now, reported AlN nanocones or similar nanostructures have mainly been formed by bottom-up growth method [12-15], but there still exists many problems in growth process, such as uncontrollability and nonuniformity, and thus the fabrication of large-area high-quality and controllable well-aligned AlN nanocone arrays has still remained as one of the foremost challenges due to technological limitation. In

addition, owing to its large direct band gap, some researchers have studied the PL properties of AlN nanostructures, however, the dependence of PL properties on the geometry-size of AlN nanostructure and related mechanism are scarcely discussed so far.

In the work, we adopted firstly a top-down method of maskless plasma etching to fabricate high-aligned AlN nanocone arrays with ordered orientation, controlled density and uniform cone angle on (002) AlN film by using hot filament chemical vapor deposition (HFCVD) system. The as-fabricated and high-aligned AlN nanocone arrays remain unchanged crystalline oriented (002) and microstructure of original AlN film, which can be served as a promising candidate for field emission (FE) and light emitters with enhanced property induced by the multiple-nanotips geometry due to their low electron affinity and large direct band gap. Compared with previously reported bottom-up growth method of the AlN nanocones [8], this top-down plasma etching method to fabricate AlN nanocone show clear superiority such as controllable morphology, good uniformity, large-area and high-throughput fabrication of nanocone arrays，providing a very simple and advantageous fabricating approach. In addition, the performing process of high-aligned AlN nanocone arrays on the silicon substrates is amenable to current technology for fabrication of Si-based microelectronics devices. The subsequent characterizations of FE and PL reveal that these AlN nanocone arrays possess a broad blue emission band and rather good FE property that can be tuned by tip-size and density of AlN nanocone, suggesting great potential applications in optoelectronics and field emission nanodevices.

2. Experimental

2.1 Preparation of (002) AlN films

The (002) AlN films were deposited on n-type (100)-oriented silicon substrates in a radio frequency (RF) magnetron sputtering system. Aluminum with 99.99% purity was used as a sputtering target. Prior to loading into the sputtering chamber, the

substrate was cleaned by dipping in a dilute solution of 4% HF for 60 s to remove the chemical surface oxide layer. Degreasing was carried out by ultrasonic-assisted cleaning in acetone and methanol. Once the base gas pressure of the chamber reached to 1 $\times 10^{-4}$ Pa, a gas flow mixture of high-purity N_2 and Ar was maintained into the chamber with a flow ratio of about 60:40. The total gas pressure was kept at 0.75 Pa during the sputtering process. The sputtering power and substrate temperature were kept at 120 W and 700 ^{o}C, respectively.

2.2 Fabrication of AlN nanocone arrays

After the growth process, the (002)-oriented AlN film with the thickness of about 800nm was placed into the HFCVD chamber with a direct current (dc) negative bias voltage for the fabrication of AlN nanocone arrays, and CH_4 and H_2 are used as etching gas. The fabrication process was based on ion sputtering, in which Ta filament in HFCVD system was heated to about 2100℃, and negative bias voltage of 300V was applied to the substrate to generate glow discharge and ion sputtering. The substrate temperature was monitored using thermocouple and modulated by changing the distance between filament and substrate. Other experimental conditions for AlN nanocone arrays formation were set as follows: the flow rate of CH_4 and H_2 is respectively in the range of 1~5 sccm and 99~95 sccm to obtain CH_4 concentration of 1%–5%, and gas pressure is kept to be 20 Torr while glow discharge current is 150mA, and the durations of ion sputtering is 1~2h.

2.3 Characterization

The surface morphology of the AlN film was characterized by scanning electron microscope (SEM), and the X-ray Diffraction (XRD) measurement was used to prove that high-quality (002)-oriented AlN films are formed at the above-mentioned experimental conditions. In addition, the AlN nanocone arrays were characterized by Transmission Electron Microscope (TEM) and EDX to observe their microstructures and components. The field emission properties for AlN nanocone arrays measurements were performed by using a conventional parallel-plate field

configuration with an anode-to-sample spacing of 200 μm (using glass fibers as spacers for all tests) under a vacuum of 2×10^{-6} Pa. The PL measurements were carried out at room temperature using a HR800 spectrometer with a 325 nm excitation of He-Cd laser.

3. Results and Discussion

The AlN films deposited on the (100)-oriented silicon wafer by RF magnetron sputtering methods, were used as a substrate for the fabrication of AlN conical nanostructure, as shown in Figure.1a. It can be seen that as- deposited AlN films display a pebble-like morphology with uniform grain size of about 20 nm in diameter, reflecting the typical surface characters of (002)-oriented AlN films that is favorable for further fabrication of the following conical structure. After a plasma etching for about 1h, uniform AlN nanocone arrays were achieved on the AlN film. As shown in Figure 1b, the SEM image of aligned AlN nanocone arrays are presented, having a high density of the nanocone of about 1×10^{9} cm^{-2} and high aspect ratio. Moreover, from the Figure 1c, we can see that the length of individual nanocone is about 600nm and the cone angle approximately of 17° , which is advantageous to tip-enhanced emission application. Figure 1d show the XRD measurement results of (002) AlN film before and after plasma etching, in which a strong diffraction peak appears at about 36° of 2θ, indicating a highly (002)-oriented character for the as-formed AlN films [16]. It is found that the intensity of the diffraction peak of AlN films is reduced due to the plasma etching process, but its location at 36° of 2θ is unchanged, verifying that plasma etching have not greatly changed the microstructure of (002) AlN film. This results indicated that as-formed AlN nanocone still remained most intrinsic property though the plasma etching might introduce the incorporation of defects.

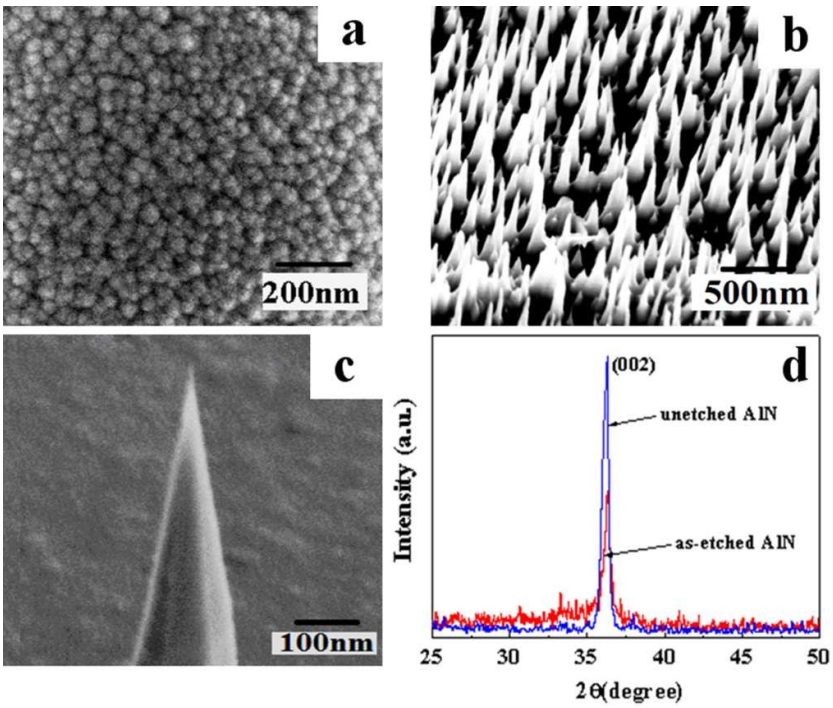

Figure 1 SEM images of (a) original (002)-oriented AlN film, (b) as-formed AlN nanocone arrays, and (c) a individual nanocone. (d) XRD measurement results of (002) AlN film before and after etching .

To further determine the detailed crystalline structure of AlN nanocone, HRTEM measurement was employed to investigate the samples. A typical TEM image of a single AlN nanotip is shown in Figure 2a, displaying a tiny apex radius and smooth surface. An amorphous layer with several nanometer is also observed on the side-wall, which is very likely be a very thin amorphous AlN layer that originates from the redeposition during etching process. Further, no any masked particles are found on the cone tip, also testifying a maskless plasma etching fabrication process. Figure 2b shows a HRTEM image of the local region of AlN nanocone, finding that the AlN nanocone has clear main atom lattice fringes and the distance spacing between the adjacent (002) plane is 0.25nm, which is in agreement with of the results of XRD measurement and presents the growth structure with a preferential growth direction

along the (002) direction. In addition, the SAED pattern shown in Figure 2c indicates that a crystal phase of AlN nanotip can be obtained, in which a preferred orientation is already seen from the arcing of the (002) diffraction spots around the growth axis, according to the occurring diffraction rings[17]. Thus it can be seen that according to this SAED pattern with very intense the diffraction spots, AlN nancone is obviously a typical of polycrystalline microstructure with well crystallite. Finally, local EDX spectroscopy analysis results in Figure 2d indicated that as-formed nanocone was composed to Al and N elements, corresponding to the AlN, and the litter O elements may be attributed to the etching process.

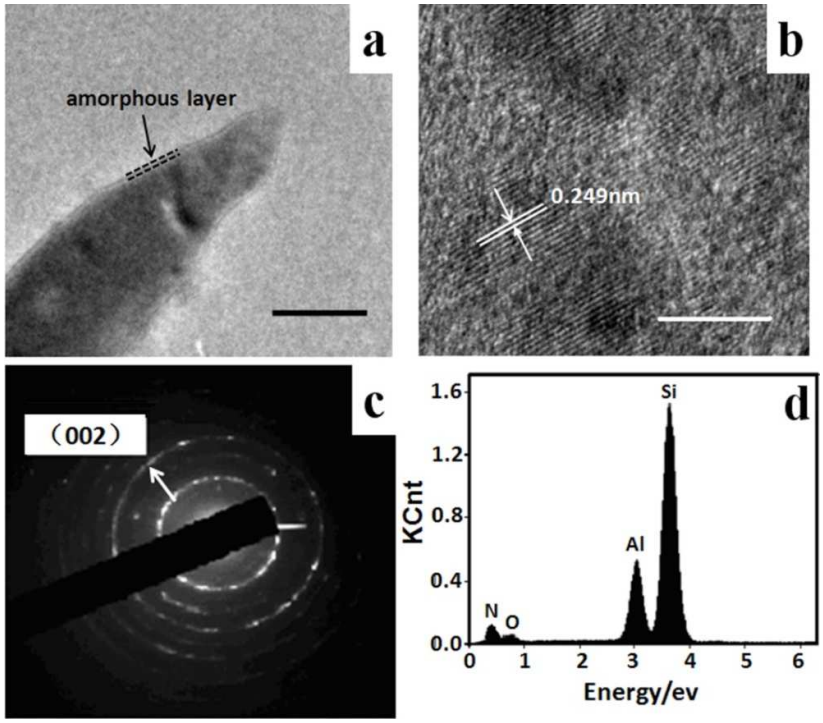

Figure 2 TEM, SEAD and EDX of a typical AlN nanocone: (a) TEM image of a single AlN nanotip. Scale bar, 40nm. (b) HRTEM image. Scale bar, 5nm (c) SEAD patterns and (d) EDX spectrum corresponding to the top region of AlN nancone.

Based on above results together with the reaction principles of the maskless selective plasma etching, a top-down formation mechanism for the AlN nanocone has been

proposed, as illustrated in Figure 3. Under the same etching condition and substrate materials, a roughness surface is more favorable to form cone-shape structure than a smooth surface, which is an effect of morphological inducing plasma etching. During plasma etching, the incident energetic ions should collide more frequently with the concave sections than the convex sections.[18] It should be noted that the particle movement is complicated and unpredictable due to the existence of the sheath field and the additional three-dimensional (3D) electric fields of random surface nanostructures, which indicates only a statistical method can be employed to provide a definite evidence to as-obtained experimental results. In the Figure 2a, a pebble-like grain can be consider as a hillock, and the different sputtering rates for different regions of the hillock are very different. If the relation of $\overline{E} > E_{th}$ ($\overline{E}$: average ion energy; and E_{th}: sputtering threshold energy) is satisfied, a sputtering of the substrate will occur. Target atoms were not usually sputtered from the exact hitting spots of the incident ions, and target atoms near the hitting spots will be sputtered out "down-stream" due to cascade-collision for low energy sputtering.[19] The sputtering rate of the cone tip is less than that of the cone bottom ($\nu_{top}<\nu_{bottom}$), and for the cones with a smaller cone angle this effect becomes more apparent. At last, certain static equilibrium among the etching of different parts will be reached, and the cones with relative height and cone angle will be developed, as shown Figure 3b-d. The real SEM images of as-formed AlN nanocone arrays are shown in Figure 3e with etching evolution, demonstrating above mechanism of morphological inducing maskless plasma etching. Therefore, the pebble-like surface structure of (002) AlN film morphologically induce plasma etching to procure the initial formation of nanocone structure so that aroused an enhanced ions sputtering effect on the pebble-like grains bases, and the nanocones structure with a larger height and smaller cone angle will be developed by further sputtering. During the formation of surface nanocones, the methylic ions play a major role in determining etching efficiency due to their much higher mean ion energies than that of H^+ ions . [18] The H^+ ions with lower

energy will result in a poor etching efficiency, but it is helpful for developing the initial surface roughness. In spite of that, a proper gas flow ratio (CH_4/H_2) should be carefully controlled during etching process, a higher gas flow rate will result in an excessive etching. In addition, other etching parameters, such as gas pressure, bias current and etching time, have an obvious effect on the morphology of as-formed AlN nanocone, which also have close relations with the mean free path and the mean energy of ions. Among these etching parameters, a lower gas pressure can increase the mean free path of ions and hence obtain a higher ion mean energy to improve etching efficiency, and thus a proper gas pressure is helpful to form the nanocone with high aspect ratio. A higher bias current can greatly enhance etching efficiency due to an increased ion current density and stable ion mean energy, and thus a reasonable control in bias current is very effective way to tune different morphologies of AlN nanocone. Finally, under an optimal etching parameters, controlling etching time becomes of great importance to a perfect etching results, by which we can obtain directly different morphologies of AlN nanocone including the density, height and tip angle of the nanocone.

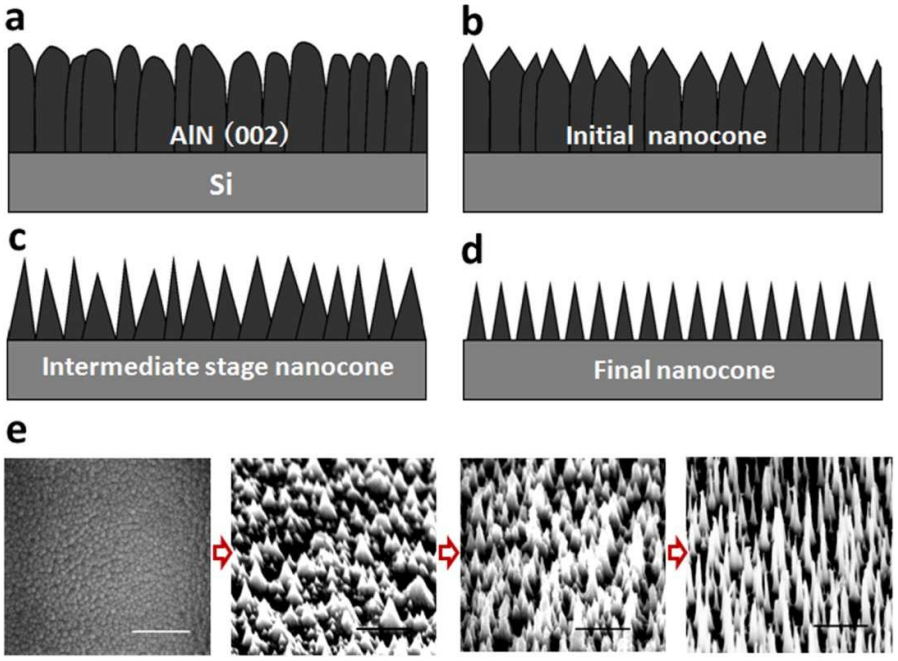

Figure 3 Illustration of morphology inducing maskless plasma etching to fabricate AlN nanocone arrays. (a) (002) AlN film with surface morphology of pebble-like grains and columnar-like cross-section before plasma etching, (b) Etching initial stage, the top of columnar-like structure become the low conical shape due to pebble-like morphology inducing selecting etching, (c) and (d) After etching duration, the size and shape of nanocone is developed to form finally discrete and uniform nanocone arrays. (e) Real SEM morphologies of AlN films and nanocone arrays corresponding to each stage of plasma etching process from (a) to (d). Scale bar, 500nm

AlN nanocone samples with different tip-sizes from ~50nm to ~10nm are selected to investigate thoroughly the effect of tip-size on PL property of AlN nanocone. Figure 4 presents the PL spectra of AlN film and nanocone arrays under the excitation wavelength of 325 nm. Compared with AlN film, AlN nanocones show a great enhancement in PL intensity, and then a reduction in tip-size of AlN nanocone can lead to a continuous improvement of the PL intensity. Despite the changes in the relative intensity of the PL bands, two broad PL bands still centered at 380 nm (3.26 eV) and 460 nm (2.7 eV), respectively, as shown in Figure 4. This means that the emission originates the same electron transition in the series of samples with the AlN film. Obviously, these two PL bands cannot be attributed to the band-to-band transitions, since AlN exhibits a wide direct band gap ~6.2 eV, corresponding to the phonon-exciton emission band around 200 nm. And, the PL bands observed in the range of 2 ~ 4 eV are generally attributed to the oxygen-related defects in the lattice structure of AlN [9]. Two oxygen atoms (O_N) substituting two nitrogen atoms and resulting in an N vacancy (V_N) lead to the different defect levels of O_N-V_{Al} complex [20]. Two prominent features in Figure 4 are worthy to be addressed here. The first one is the significant enhancement of the PL bands for the AlN nanocone arrays, compared with that of the AlN film. The enhanced PL band centered at 380 nm has

been observed in AlN nanowires, nanotips and nanopyramids [13-15]. According to Berzina *et al.* classification, the 380 nm band originates from the excitations of the O_N-V_{Al} complex to the separated O_N ion level [21]. On the other hand, the relative weak band around 460 nm has also been observed in other AlN nano-materials, such as nanocrystal and nanotubes, which is attributed to the vacancies of N [22]. Secondly, it is striking to find that the PL intensities increase with the decrease of the apex radius of the cones, especially for the nanocones with average apex radius of 10 nm, of which the PL intensity is thirty times stronger than that of AlN film. It is generally accepted that the PL intensity of the semiconductors increase when their size decrease to the nanometer scale due to the increasing surface defects and oxygen impurities that increase the recombination rate of the phonon-induced electron-hole pairs[23]. Torchynska has demonstrated that the PL intensity increases with decreasing the grain size of Si nano-crystallites [24]. The enhancement of the 380 and 460 nm PL bands for the AlN nanocone arrays may be associated with the increased luminance centers that arise from the etching process. The longer the etching time, the smaller the nanocones, and the higher defect density on the cone surface. In addition, the surface defects of the cones also improve the light excitation efficiency [25]. The nanocone structures assist the photons with multiple opportunities to escape from the wafer surface and redirect the photons which are originally emitted out of the escape cone back into the escape cone [26]. The intense PL emission in the range of 2-4 eV indicates that the well-aligned AlN cones would have potential application in light emission nanodevices.

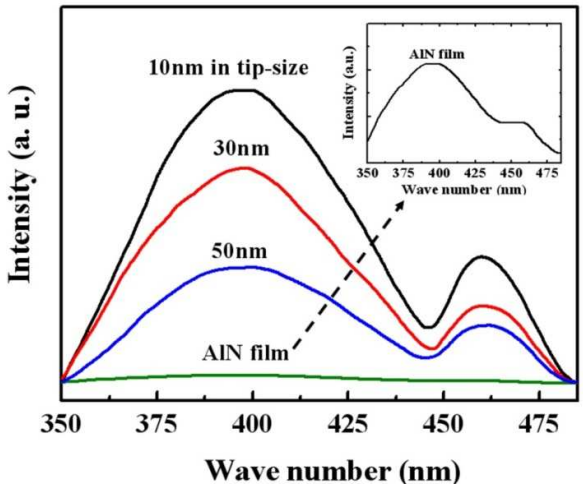

Fig.4 PL curves of AlN film and nanocone with various apex radiuses: 10nm, 30nm, 50nm, and an inserted and enlarged PL spectrum of AlN film.

To further evaluate the feasibility of applying AlN in the vacuum nanoelectronic fields, we have measured the FE properties of AlN nanocone arrays with various cone densities, as shown in Figure 5. Three kinds of nanocone samples were selected from many samples used as field emitters, which have a similar morphology of cone height and cone angle but different cone densities, corresponding to 1×10^9， 5×10^8 and 8×10^7 /cm^2, respectively. From the J-E curve of AlN nanocone arrays and film (Figure 5a), we found that the emission current density of nanocone array is greatly higher than the film at the same applied electric field, which is mainly attributed to the nanotip-geometrical enhancement effect of the nanocones. In order to compare the FE capability of above three kinds of nanocone arrays with different densities, their turn-on fields (defined as turn-on field for 10μA/cm^2) were measured to be 5.6V/μm, 3.2 V/μm, and 7.9 V/μm, respectively. The current densities of these nanocone arrays were measured to be 145μA/cm^2, 352μA/cm^2, and 22μA/cm^2 when the electric field is kept at 8V/μm. It is clear indicated that the AlN nanocone array sample with a density of 5×10^8 /cm^2 has the best FE characteristic among three samples with different densities. The results indicate that local field electron emission ability can be observably increased with increasing the number of nanocones density. More nanocones may provide a large number of emitting sites to contribute the electron tunneling enhancement for electron emission. Nevertheless, overmuch nancones distribution will bring field shield effects that results in the reduction of FE property. Thus, we can conclude that a proper AlN nanocone density can enhance greatly the electron emission property. In addition, compared with reported results of as-grown AlN nanostructures[27-29], AlN nanocone array fabricated by maskless plasma etching here has a better FE property with more low turn on filed and high current density. A good morphological controllability and high uniformity of as-formed AlN

nanocone arrays in this work can optimize effectively the emission site density and emission stability, and their high aspect ratio and tiny-tips may increase greatly field enhancement factor for improving electron emission ability. In addition of the density, the apex angle and conductivity of the nanocone have a considerable influence on their FE properties. In this work, we concerned primarily the effect of nanocone density on the FE property because the FE ability is greatly dependent on the density of emission site that is determined mainly by the density of the nanocone.

The corresponding Fowler-Nordheim (FN) plots of AlN nanocone arrays with different densities and AlN film were shown in Figure 5b. The linearity of four curves indicate that their FE process follows FN theory, and the measured current is apparently due to the FE. According to the FN equation, if we assumed a constant work function of 3.7eV, the field enhancement factor of various densities of cone arrays could be estimated to be 286, 484, and 402 by the FN equation and FN plot slope, respectively [30]. These values imply that 5×10^8 /cm^2 nanocone arrays has a bigger field enhancement factor than that of 1×10^9 and 8×10^7 /cm^2 nanocone arrays. Otherwise, the emission stability was tested for about 1h at a constant electric field. No visible degradation of current density was observed. Therefore, our results proved that as-fabricated AlN nanocone arrays have very excellent and stable FE property, and plasma etching to fabricate AlN nanocone is a promising route for the practical application of AlN-based field emitters.

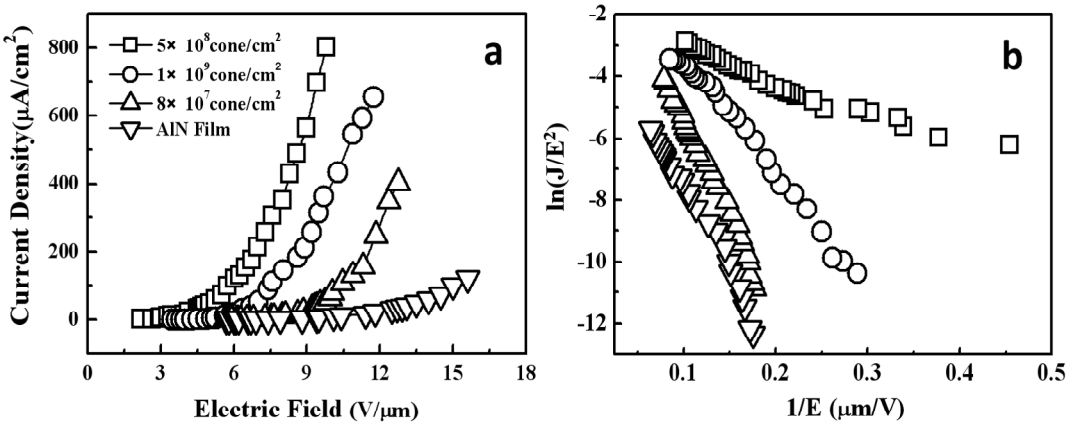

Fig.5 Field emission J-E curve of AlN nanocone arrays with different densities (a) and corresponding to FN plots (b).

4. Conclusions

In summary, vertically aligned AlN nanocone arrays with controlable densities and tip-sizes have been successfully fabricated by using top-down plasma etching method. A morphology inducing selective plasma etching process is developed to fabricate lager-area AlN nanocone arrays without any masked process. As-fabricated AlN nanocones showed a great enhancement in PL and FE properties, depending on the tip-size of AlN nanocones. With decreasing apex radius of the cones, the PL intensities of AlN nanocone arrays are increased gradually, which is due to the formation of the high-density nanocone structures with rich surface defects and oxygen impurities induced by plasma etching that increase the recombination rate of the phonon-induced electron-hole pairs. The FE results indicate that high densities and tip-effect of AlN nanocone arrays lead to their good field emission ability, and more nanocones may provide a large number of emitting sites to contribute the electron tunneling enhancement, but too dense nanocones make against the increase of FE due to a field shield effects. Therefore, this morphology inducing selective plasma etching method provide a very simple and effective approach to fabricate AlN nanocone arrays with reliable controllability and uniformity as well as high-throughput for further practical application of AlN-based nanodevices in optoelectronics and nanoelectronics field.

Acknowledgements

The authors acknowledge the National Natural Science Foundation of China (Grand No. 11174362, 91023041, 51272278, 61390503), and the Knowledge Innovation Project of CAS (Grand No. KJCX2-EW-W02).

Notes and references

1. S. Nakamura and G. Fasol, The Blue Laser Diode (Springer. Heidellberg, **1997**).

2. M. C. Benjamin, C. Wang, R. F. Davis and R. J. Nemanich, *Appl. Phys. Lett.*, 1994, **64**, 3288.

3. Y. Taniyasu, M. Kasu, and T. Makimoto, *Nature*, 2004, **44**, 325.

4. C. Liu, Z. Hu, Q. Wu, X.Z. Wang, Y. Chen, H. Sang, J.M. Zhu, S.Z. Deng and N.S. Xu, *J. Am. chem. Soc*., 2005,**127**,1318.

5. Y. B. Tang, H. T. Cong, Z. G. Zhao and H. M. Cheng, *Appl. Phys. Le*tt., 2005, **86,** 153104.

6. L.W. Yin, Y. Bando, Y.C. Zhu, M.S. Li, C.C. Tang and D. Golberg, *Adv.Mater*. , 2005, **17,** 110.

7. S. C. Shi, C. F. Chen, S. Chattopadhyay, Z. H. Lan, K. H. Chen and L. C. Chen, *Adv. Funct. Mater*.**,** 2005, **15**, 781.

8. Y.L. Li, C.Y. Shi, J.J. Li, and C.Z. Gu, *Applied Surface Science*, 2008,**254,** 4840.

9. J. H. He, R. Yang, Y. L. Chu, L.J. Chou, L. J. Chen and Z. L. Wang. *Adv.Mater*., 2006, **18**, 650.

10. G.Y. Wang, X. Jiang and E.G. Wang, *Science*, 2003, **300,** 472.

11. Q. Wang, Z. L. Wang, J. J. Li, Y. Huang, Y. L. Li, C. Z. Gu and Z. Cui, *Appl. Phys. Lett*., 2006**, 89**,063105.

12. W. M. Yim, E. J. Stofko, P. J. Zanzucchi, J. I. Pasnkove, M. Ettehberg and S. L. Gilbert, *J. Appl. Phys*., 1973,**44**, 292.

13. C. Xu, L. Xue, C. Yin, and G. Wang, *phys. stat. sol. (a)* ,2003,**198**, 329.

14. S. C. Shi, C. F. Chen, S. Chattopadhyay, K. H. Chen, B. Ke, L. Chen, L, Trinkler and B. Berzina, *Appl. Phys. Lett*., 2006, **89**, 163127.

15. J. Zheng, X. Song, B. Yu, and X. Li, *Appl. Phys. Lett.*, 2007, **90**, 193121.

16. H. Okano, Y. Takahashi, T. Tanaka, K. Shibata and S Nakano, *Japanese Journal Of Applied Physics Part 1*, 1992**, 31**, 3446.

17. J.X. Zhang, Y.Z. Chen, H. Cheng, A. Uddin, Shu Yuan, K. Pita and T.G. Andersson,

Thin Solid Films, 2005, **471**,336.

18. Q. Wang, C. Z. Gu ,Z. Xu, J. J. Li, Z. L. Wang, X.D. Bai and Z. Cui, *J. Appl. Phys*., 2006,**100**, 034312.

19. J. Zhou, I. T. Martin, R. Ayers, E. Adams, D. Liu and E. R. Fisher, *Plasma Sources Sci. Technol.*, 2006, **15**, 714.

20. S. Schweizer, U. Rogulis, J.-M. Spaeth, L. Trinkler and B. Berzina, *Phys. Stat. Sol. B*, 2000,**219**, 171.

21. B. Berzina, L. Trinkler, J. Sils, K. Atobe and Radiat, *Eff. Defects Solids*, 2002**, 157**, 108.

22. T. Xie, X. Y. Yuan, G. S. Wu, Y. Lin,X. X. Xu, G. W. Meng and L. D. Zhang, *J. Phys.: Condens. Matter*, 2004, **16,** 1639.

23. S. Bellucci, A.I. Popov, C. Balasubramanian, G. Cinque, A. Marcelli, I. Karbovnyk, V. Savchyn and N. Krutyak, *Radiation Measurements*, 2007, **42**, 708.

24. T. V. Torchynska, *Phys. Stat. Sol. C*, 2007, **4,** 375.

25. D. W. Kim, H. Y. Lee, M. C. Yoo and G. Y. Yeom, *Appl. Phys. Lett.*, 2005, **86**, 052108.

26. C. B. Soh, B. Wang, S. J. Chua, K. X. Lin, J. N. Tan and S. Tripathy, *Nanotechnology*, 2008, **19**, 405303.

27. W.J. Qian, H.W. Lai, X.Z. Pei, J. Jiang, Q. Wu, Y.L. Zhang, X.Z. Wang and Z. Hu, *J. Mater. Chem.*, 2012, **22**, 18578–18582

28. X. H. Ji, Q. Y. Zhang, S. P. Lau, H. X. Jiang and J. Y. Lin, *Appl. Phys. Lett.*, 2009, **94**, 173106-8.

29. W.J. Qian, Y.L. Zhang, Q. Wu, C.Y. He, Y. Zhao, X.Z. Wang and Z. Hu, *J. Phys. Chem. C.* , 2011, **115**, 11461-5.

30. J.J. Li, C.Z. Gu, Q. Wang, P. Xu, Z.L. Wang, Z. Xu and X.D. Bai, *Appl . Phys. Lett.*, 2005, **87**, 143107-9.

Uniform AlN nanocone arrays with enhanced photoluminescence and field emission properties are controllably fabricated by morphology inducing selective plasma etching.